AMERICAN SOCIETY FOR MICROBIOLOGY | Molecular and Cellular Biology®

RESEARCH ARTICLE

RBM4 Regulates Neuronal Differentiation of Mesenchymal Stem Cells by Modulating Alternative Splicing of Pyruvate Kinase M

Chun-Hao Su,[a,b] Kuan-Yang Hung,[b] Shih-Chieh Hung,[b,c,d] Woan-Yuh Tarn[a,b]

Institute of Molecular Medicine, College of Medicine, National Taiwan University, Taipei, Taiwan[a]; Institute of Biomedical Sciences, Academia Sinica, Taipei, Taiwan[b]; Department of Orthopedics, Integrative Stem Cell Center, China Medical University Hospital, Taichung, Taiwan[c]; Graduate Institute of Clinical Medical Science, China Medical University, Taichung, Taiwan[d]

ABSTRACT RBM4 promotes differentiation of neuronal progenitor cells and neurite outgrowth of cultured neurons via its role in splicing regulation. In this study, we further explored the role of RBM4 in neuronal differentiation. During neuronal differentiation, energy production shifts from glycolysis to oxidative phosphorylation. We found that the splice isoform change of the metabolic enzyme pyruvate kinase M (PKM) from PKM2 to PKM1 occurs during brain development and is impaired in RBM4-deficient brains. The PKM isoform change could be recapitulated in human mesenchymal stem cells (MSCs) during neuronal induction. Using a PKM minigene, we demonstrated that RBM4 plays a direct role in regulating alternative splicing of PKM. Moreover, RBM4 antagonized the function of the splicing factor PTB and induced the expression of a PTB isoform with attenuated splicing activity in MSCs. Overexpression of RBM4 or PKM1 induced the expression of neuronal genes, increased the mitochondrial respiration capacity in MSCs, and, accordingly, promoted neuronal differentiation. Finally, we demonstrated that RBM4 is induced and is involved in the PKM splicing switch and neuronal gene expression during hypoxia-induced neuronal differentiation. Hence, RBM4 plays an important role in the PKM isoform switch and the change in mitochondrial energy production during neuronal differentiation.

KEYWORDS alternative splicing, hypoxia, mesenchymal stem cells, neuronal differentiation, pyruvate kinase M

Received 18 August 2016 **Returned for modification** 9 September 2016 **Accepted** 1 November 2016

Accepted manuscript posted online 7 November 2016

Citation Su C-H, Hung K-Y, Hung S-C, Tarn W-Y. 2017. RBM4 regulates neuronal differentiation of mesenchymal stem cells by modulating alternative splicing of pyruvate kinase M. Mol Cell Biol 37:e00466-16. https://doi.org/10.1128/MCB.00466-16.

Copyright © 2017 American Society for Microbiology. All Rights Reserved.

Address correspondence to Woan-Yuh Tarn, wtarn@ibms.sinica.edu.tw.

The splicing regulator RBM4 modulates alternative splicing of a number of transcripts involved in cell differentiation and tumorigenesis (1, 2). Previous studies demonstrated the role of RBM4 in differentiation of muscle and pancreas cells and adipocytes (3–5). We recently reported that RBM4 is also involved in neuronal differentiation of mouse embryonal carcinoma P19 cells and neural progenitor-derived cells (1). RBM4 promotes the expression of Numb splice isoforms that function during neuronal differentiation as well as neurite outgrowth. Mesenchymal stem cells (MSCs) are adult bone marrow stromal cells that can differentiate into a variety of cell types, including neurons, and have potential in regenerative therapy for neurological diseases (6). In this study, we assessed whether RBM4 can also modulate neuronal differentiation of MSCs and explored the underlying mechanism.

Cellular energy metabolism undergoes a dynamic change during development. In principle, anabolic glycolysis dominates in embryonic stem cells and permits rapid cell proliferation similar to that in cancer cells (7, 8). Most adult stem cells exhibit low glycolysis activity in a quiescent state and undertake active glycolysis while proliferat-

ing (7–9). Upon cell differentiation, glycolytic flux drops rapidly so that the energy pathway switches from glycolysis to oxidative phosphorylation (OXPHOS) (10–12). Such a metabolic switch may also be important for cell cycle exit and cell fate determination. In *Drosophila melanogaster*, upregulation of OXPHOS is required for terminal differentiation of neural stem cells (13). In the developing mammalian cortex, oxygen tension suppresses radial glia expansion but induces neuronal cell differentiation (14). Analogously, suppression of oxidative metabolism in human gliomas resumes neural stem cell proliferation (15). Moreover, neurons and astrocytes exhibit distinct metabolic pathways, i.e., OXPHOS and glycolysis, respectively (16). Therefore, metabolic reprogramming influences not only cell cycle progression but also cell specification or terminal differentiation.

A transcriptome profiling study indicated that neurons and astrocytes in the mouse cerebral cortex exhibit different expression profiles for glycolytic genes, including the pyruvate kinase M (PKM) gene (17). The metabolic reconfiguration involves a switch in the expression of the splice isoforms of PKM (PKM1 and PKM2) via mutually exclusive selection of exon 9 (PKM1) or 10 (PKM2). PKM2 is expressed in embryonic and tumor cells. PKM2 contributes to intricate metabolic reprogramming via the monomer-dimer-tetramer interconversion, and it also can transcriptionally modulate gene expression (18). In contrast, PKM1 essentially promotes OXPHOS in energy-consuming tissues, such as brain and muscle (19). The PKM isoform switch correlates with metabolic changes during myoblast differentiation into myotubes (20). The splicing factors hnRNP A1/A2 and PTB promote PKM2 expression by suppressing exon 9 inclusion, and their expression levels are modulated by oncogenic pathways in cancer, leading to increased PKM2 levels (21). Nevertheless, how PKM splicing is regulated during development remains largely unknown.

In this study, we characterized RBM4-mediated PKM1 induction during neuronal differentiation of MSCs. Unexpectedly, we found that RBM4 induces a specific PTB isoform in MSCs and that RBM4 is induced in response to hypoxia to modulate the PKM splicing switch.

RESULTS

RBM4 is critical for alternative splicing of PKM pre-mRNA during brain development. PKM1 is expressed in energy-consuming tissues, including brain and skeletal muscle, whereas PKM2 is expressed more dominantly in embryonic cells (19). We previously observed a change in expression of Pkm isoforms, i.e., from Pkm2 to Pkm1, during neuronal differentiation of mouse embryonal carcinoma P19 cells (1). We thus further explored the significance and mechanism of this isoform switch during development. Total RNAs isolated from mouse tissues at embryonic day 13.5 (E13.5) to E18.5 were analyzed by reverse transcription-PCR (RT-PCR) using primers specific to Pkm1 or Pkm2 (Fig. 1A). The results showed a gradual change from Pkm2 to Pkm1 in the developing mouse brain as well as in other tissues, albeit to different extents (Fig. 1B). RBM4 expression levels also increased during the period examined (Fig. 1B, immunoblotting [IB] panel). Next, we examined Pkm isoform expression in RBM4-deficient (i.e., *Rbm4a* or *Rbm4b* knockout) mouse brains. Compared to the levels for wild-type littermates, the level of Pkm2 increased in either *Rbm4* knockout brain at E13.5 (Fig. 1C), suggesting that RBM4 may be important for the Pkm isoform switch during brain development. However, splicing differences between the wild type and the *Rbm4* single-gene knockouts were insignificant after E15.5 (see Fig. S1A in the supplemental material), perhaps because one *Rbm4* gene could compensate for the loss of another gene.

RBM4 regulates alternative splicing of PKM pre-mRNA via an intronic CU-rich sequence. To examine the role of RBM4 in regulating alternative splicing of PKM pre-mRNA, we established a mouse PKM minigene spanning exons 8 to 11 (Fig. 2A). This minigene was cotransfected with a FLAG-RBM4 expression vector into HEK293T cells. The results showed that the splicing switch from PKM2 to PKM1 correlated with RBM4 expression in a dose-dependent manner (Fig. 2B). Because RBM4 overexpression

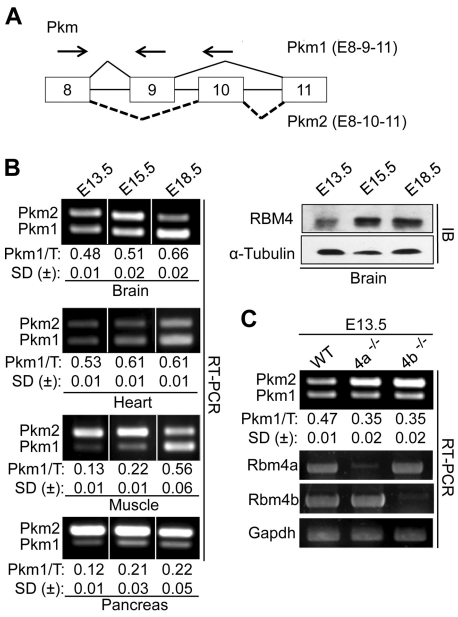

FIG 1 RBM4 is involved in the splice isoform change of Pkm during mouse brain development. (A) Schematic diagram of alternative splicing of the mouse Pkm gene. Arrows depict the primers used for RT-PCR (see Table S1 in the supplemental material). (B) Total RNA was extracted from the indicated mouse tissues at the indicated embryonic days and subjected to RT-PCR analysis using primers as depicted in panel A. Representative lanes were spliced from the original gels (Fig. S1A and B). The right panel shows immunoblotting of RBM4 in embryonic brain lysates. (C) RT-PCR was performed on wild-type and *Rbm4a* or *Rbm4b* knockout embryonic brains at E13.5 to detect the expression of Pkm isoforms (spliced from an original gel shown in Fig. S1A), Rbm4a, Rbm4b, and Gapdh (as a control). For all panels, ratios of Pkm1 to total Pkm transcripts (T) are shown below the gels; the average values and standard deviations (SD) were obtained from 2 or 3 sets of samples.

downregulates PTB expression (3), the argument remained that RBM4 influences PKM splicing merely by suppressing PTB expression. However, we found that a low dose of FLAG-RBM4 (0.05 μg) did not suppress PTB expression (Fig. 2C), whereas at this dose or lower doses, RBM4 was sufficient to induce the switch from PKM2 to PKM1 (compare the data for the 0.05-μg dose in Fig. 2B and C), suggesting that RBM4 regulates PKM splicing directly, not likely through suppression of PTB levels.

A previous report indicated that PTB suppresses exon 9 usage of human PKM via binding of two UCUU motifs upstream of the 3′ splice site of intron 8 (22). RBM4 also has a preference for CU-rich sequences (23). A CU-rich sequence in mouse PKM gene intron 8 is similar but not identical to its human counterpart. To examine whether such a sequence is responsible for RBM4-mediated splicing regulation, we first performed an electrophoretic mobility shift assay (EMSA). Figure 2D shows that a recombinant maltose binding protein (MBP)-RBM4 fusion bound to the ^{32}P-labeled CU-rich PKM intron probe (Fig. 2A) but not to the CU-poor control. Next, we generated a CU-rich sequence-truncated minigene. This mutant minigene had a lower capacity for PKM1 expression (Fig. 2E, compare lanes 1 and 4). RBM4 hardly induced PKM1 splicing in the mutant (Fig. 2E), suggesting that RBM4 modulates PKM splicing via binding to the CU-rich sequence in intron 8. However, PTB still promoted the PKM2 isoform choice in the mutant (Fig. 2E). When RBM4 and PTB were both overexpressed with the PKM minigene, a high dose of RBM4 could counteract the effect of overexpressed PTB on PKM2 induction (Fig. 2F). Thus, RBM4 antagonizes the activity of PTB as previously reported (3, 23).

RBM4 is involved in the PKM isoform switch during neuronal differentiation of human MSCs. Differentiation of human MSCs into osteoblasts involves a metabolic change from glycolysis to OXPHOS (12). We therefore explored whether the PKM isoform switch occurs during MSC differentiation into neuronal cells and whether RBM4 is involved in primary human MSCs and derived 3A6 cells (24). Cells were cultured in

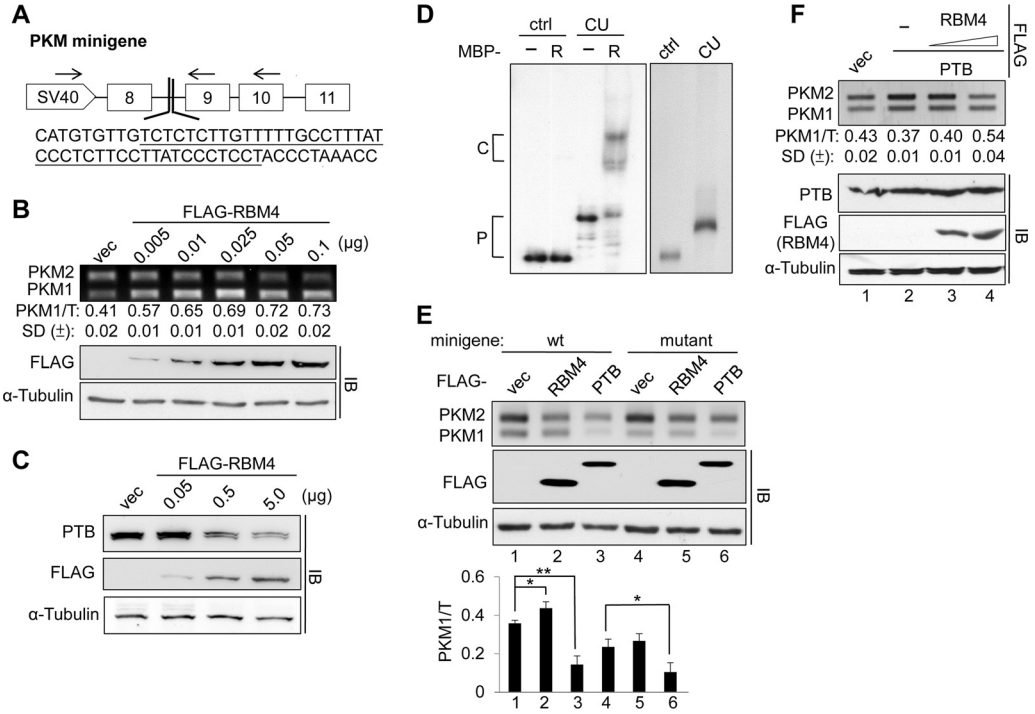

FIG 2 RBM4 regulates alternative splicing of PKM via an intronic CU-rich sequence. (A) Schematic diagram of the PKM minigene spanning exons 8 to 11 of mouse Pkm. A CU-rich region (61 nt) in intron 8 was used as a probe for EMSA; the underlined region (42 nt) was deleted in the mutant reporter. Arrows depict primers used for RT-PCR (see Table S1 in the supplemental material). SV40, simian virus 40. (B) HEK293T cells were transfected with the indicated amounts of the FLAG-RBM4 expression vector or empty vector (0.1 μg) (vec). (C) HEK293T cells were transfected with the indicated amounts of the FLAG-RBM4 expression vector or empty vector (5.0 μg). (D) For EMSA, a ^{32}P-labeled control or CU-rich probe was incubated with recombinant MBP (−) or MBP-RBM4 (R) and then analyzed by nondenaturing polyacrylamide gel electrophoresis. C, RNA-protein complex; P, free probe. (E) HEK293T cells were cotransfected with an expression vector (empty, 0.1 μg of FLAG-RBM4, or 0.5 μg of FLAG-PTB) and the PKM minigene (wild type or mutant). The bar graph shows ratios of PKM1 to total PKM; the averages and standard deviations were obtained from three experiments. *, $P < 0.05$; **, $P < 0.01$. (F) The PKM minigene was cotransfected with empty vector (lane 1) or 1 μg of the FLAG-PTB vector and 0, 1, or 2 μg of the FLAG-RBM4 vector (lanes 2 to 4) into HEK293T cells. For panels B, E, and F, the ratios of PKM1 to total PKM were calculated as described in the legend to Fig. 1. The average values and standard deviations were obtained from three independent experiments. Immunoblotting (IB) was performed using antibodies against PTB, α-tubulin, and the FLAG tag.

neuronal induction medium (NIM) for up to 7 days. The results revealed the change from PKM2 to PKM1 and an increase in RBM4 level during differentiation of both cell types (Fig. 3A and B). Differentiation of 3A6 cells was further demonstrated by increased expression of several neuron-associated genes, including those encoding neuron-specific class III β-tubulin (TUJ1), microtubule-associated protein 2 (MAP2), synuclein alpha (SNCA), and nuclear receptor subfamily 4 group A member 2 (NR4A2/NURR1), as well as by an increase in the Tuj1 protein level (Fig. 3B).

Next, we assessed whether the RBM4 level affects alternative splicing of PKM in MSCs. We depleted endogenous RBM4 by using a small interfering RNA (siRNA) or transiently overexpressed FLAG-tagged RBM4 in 3A6 cells. Depletion of RBM4 increased PKM2 expression, whereas overexpression of FLAG-RBM4 promoted the production of PKM1 (Fig. 3C). Finally, we performed FLAG-RBM4 immunoprecipitation followed by RT-PCR analysis. The results showed that PKM mRNA was coprecipitated with FLAG-RBM4 in 3A6 cells (Fig. 3D). All these results indicated that RBM4 participates in the PKM splicing switch during neuronal differentiation of MSCs.

RBM4 induces the expression of a PTB isoform with attenuated splicing activity in human MSCs. RBM4 promotes the expression of the exon 11-skipping PTB mRNA isoform and thereby downregulates PTB expression via nonsense-mediated mRNA decay (NMD) in various cell types (3, 5). We wondered whether RBM4 also reduces PTB expression during neuronal differentiation of MSCs. In 3A6 cells, exon 11 skipping of PTB mRNA was not readily detected even in the presence of cycloheximide (CHX) and

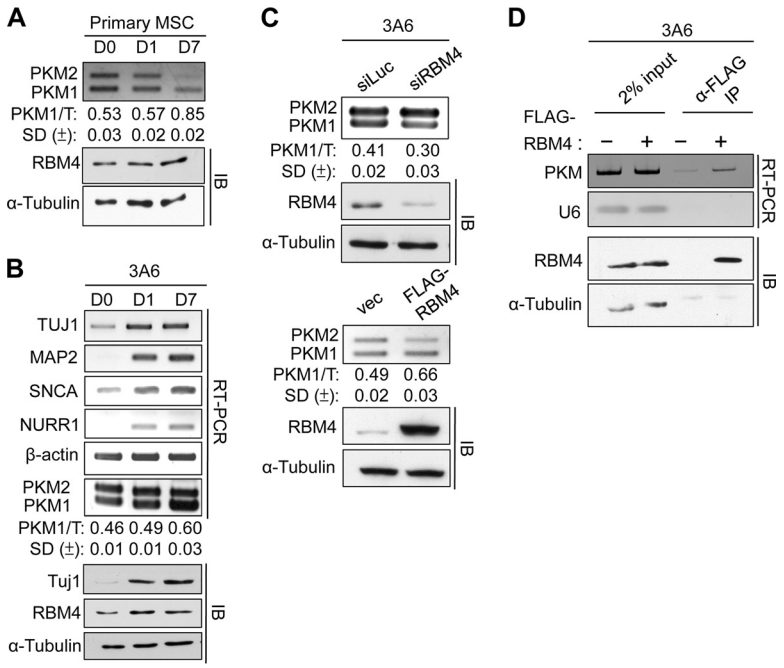

FIG 3 RBM4 regulates the splice isoform switch of PKM during neuronal differentiation of MSCs. (A and B) Primary human mesenchymal stem cells (MSCs) (A) or 3A6 cells (B) were cultured in neuronal differentiation medium for up to 7 days (D0 to D7). The expression of neuronal genes was detected by RT-PCR using specific sets of primers (see Table S1 in the supplemental material). (C) 3A6 cells were transfected with siRBM4 (or siLuc as a control) or with the FLAG-RBM4 or empty expression vector for 2 days or 30 h, respectively. For panels A to C, the PKM isoforms were detected and relative ratios calculated as described in the legend to Fig. 1A, except that human PKM primers were used. Immunoblotting (IB) was performed using antibodies against Tuj1, RBM4, and α-tubulin. (D) Mock-transfected or FLAG-RBM4-expressing 3A6 cell lysates were subjected to immunoprecipitation (IP) using anti-FLAG. RT-PCR was performed to detect coprecipitated PKM transcripts. U6 snRNA was used as a control.

was induced very minimally by RBM4 overexpression, unlike observations in mouse myoblast C2C12 cells (Fig. 4A, data for PTB-4^{-e11} and PTB-1^{-e11}). Nevertheless, the observation that RBM4 overexpression slightly induced exon 9 skipping of PTB in 3A6 cells (Fig. 4A, lane 2) was reminiscent of a recent report that the exon 9-skipping isoform of PTB (PTB-1) is induced during neuronal differentiation of mouse embryonic stem cells (25). We indeed observed that exon 9 skipping of PTB increased gradually during neuronal differentiation of primary MSCs (Fig. 4B, RT-PCR panel). Immunoblotting with anti-PTB confirmed the change from the exon 9-containing isoform to the exon 9-skipping isoform (Fig. 4B, IB panel). RBM4-induced exon 9 skipping was observed in 3A6 cells and, even more robustly, in HeLa and HEK293T cells (Fig. 4C, RT-PCR panels). Accordingly, RBM4 overexpression raised the PTB-1 protein level, albeit minimally (Fig. 4C, IB panels). Under these conditions, the overall PTB protein level was not reduced, unlike that observed in other cell types (Fig. 2) (3, 5). With all these data, we provide evidence that RBM4 induces a PTB protein isoform, PTB-1, in MSCs without affecting the overall PTB level.

Next, we generated a PTB minigene spanning exons 8 to 10 and performed an *in vivo* splicing assay in both 3A6 and HEK293T cells. The result confirmed the activity of RBM4 in promoting exon 9 skipping (Fig. 4D). Immunoprecipitation and RT-PCR demonstrated the association of FLAG-RBM4 with endogenous PTB transcripts in 3A6 cells (Fig. 4E), emphasizing the direct role of RBM4 in the splicing or biogenesis of PTB transcripts.

Finally, we assessed whether PTB-1 and PTB-4 exhibit different activities in PKM splicing. Using the minigene assay, we observed that both isoforms could reduce the ratio of PKM1 to total PKM (Fig. 4F). PTB-4 appeared to have a higher activity than that of PTB-1, as recently reported (25).

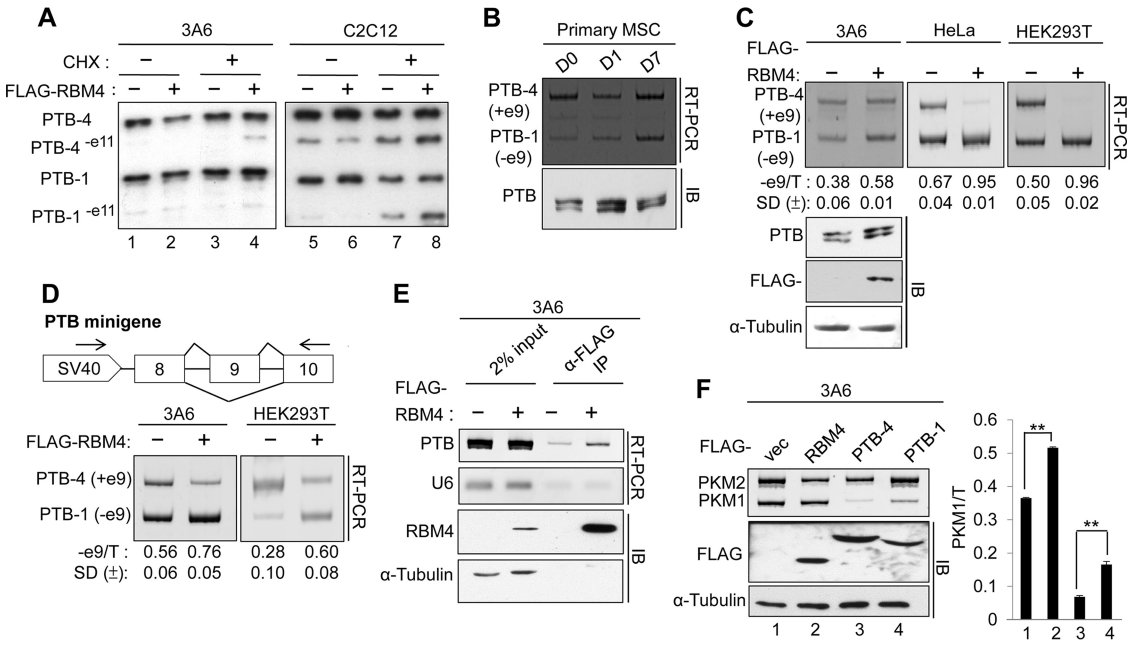

FIG 4 RBM4 modulates PTB isoform expression during neuronal differentiation of MSCs. (A) 3A6 cells or C2C12 myoblasts were transfected with the empty or FLAG-RBM4 expression vector. At 30 h posttransfection, cells were mock treated or treated with 100 μM cycloheximide (CHX) for 2 h before being harvested. Total RNA was subjected to RT-PCR analysis using primers specific for exons 8 and 12 of human PTB (Table S1). (B) Primary human MSCs were cultured as described in the legend to Fig. 3A. Total RNA was analyzed using primers as described for panel A. Immunoblotting (IB) was performed using anti-PTB. (C) 3A6 cells, HeLa cells, and HEK293T cells were transfected as described for panel A. RT-PCR was performed as described for panel B. Immunoblotting was performed using anti-PTB, anti-FLAG, and anti-α-tubulin. (D) Schematic diagram of the PTB minigene spanning exons 8 to 10 of human PTB. 3A6 cells and HEK293T cells were cotransfected with the expression vector (empty or FLAG-RBM4) and the PTB minigene. PTB isoform expression was detected by RT-PCR using specific primers as depicted. Ratios of PTB−e9 (PTB-1) to total PTB are shown below the gels; averages and standard deviations were obtained from three independent experiments. (E) Immunoprecipitation was performed as described in the legend to Fig. 3D, followed by RT-PCR using PTB primers. U6 snRNA was used as a control. (F) The PKM minigene was transfected with empty vector or a vector expressing FLAG-RBM4 or FLAG-PTB-4 (+e9) or -PTB-1 (−e9). RT-PCR and immunoblotting were performed. The bar graph shows ratios of PKM1 to total PKM (n = 3).

RBM4 promotes neuronal differentiation by upregulating the expression of neuron-associated genes. We assessed whether RBM4 could promote neuronal differentiation of MSCs. Using 3A6 cells, we observed that overexpression of FLAG-RBM4 significantly upregulated the expression of neuronal genes in noninduced cells (Fig. 5A). In contrast, the expression of two stemness genes, the OCT4 and SOX2 genes, and one proliferation-related gene, the HES1 gene, was downregulated by RBM4 (Fig. 5A). To further evaluate the role of RBM4 in neuronal differentiation, we took advantage of a quantitative PCR-array analysis of RBM4-overexpressing 3A6 cells. We observed and confirmed that the level of bone morphogenetic protein 2 (BMP2) was reproducibly downregulated in several independent experiments (Fig. 5B). Accordingly, the expression of the BMP2 downstream target DNA-binding protein inhibitor 1 (Id1) was reduced or increased upon overexpression or knockdown, respectively, of RBM4 (Fig. 5B). Both BMP2 and Id1 have negative roles in neuronal differentiation (26). Therefore, RBM4 may downregulate the BMP-Id1 pathway to promote neuronal differentiation of MSCs.

Next, we examined cell morphological changes of RBM4-overexpressing cells. By immunofluorescence staining for Tuj1, we observed only a small proportion of RBM4-overexpressing 3A6 cells that could generate neurites under noninduced conditions. Nevertheless, when cells were cultured under differentiation conditions, we observed that RBM4 overexpression considerably promoted neurite outgrowth (Fig. 5C). Finally, we depleted RBM4 in 3A6 cells cultured under differentiation conditions. RBM4-deficient cells exhibited delayed or reduced expression of the neuronal markers TUJ1 and MAP2 (Fig. 5D). These results further suggested that RBM4 plays an important, though not initiating, role in promoting neuronal differentiation.

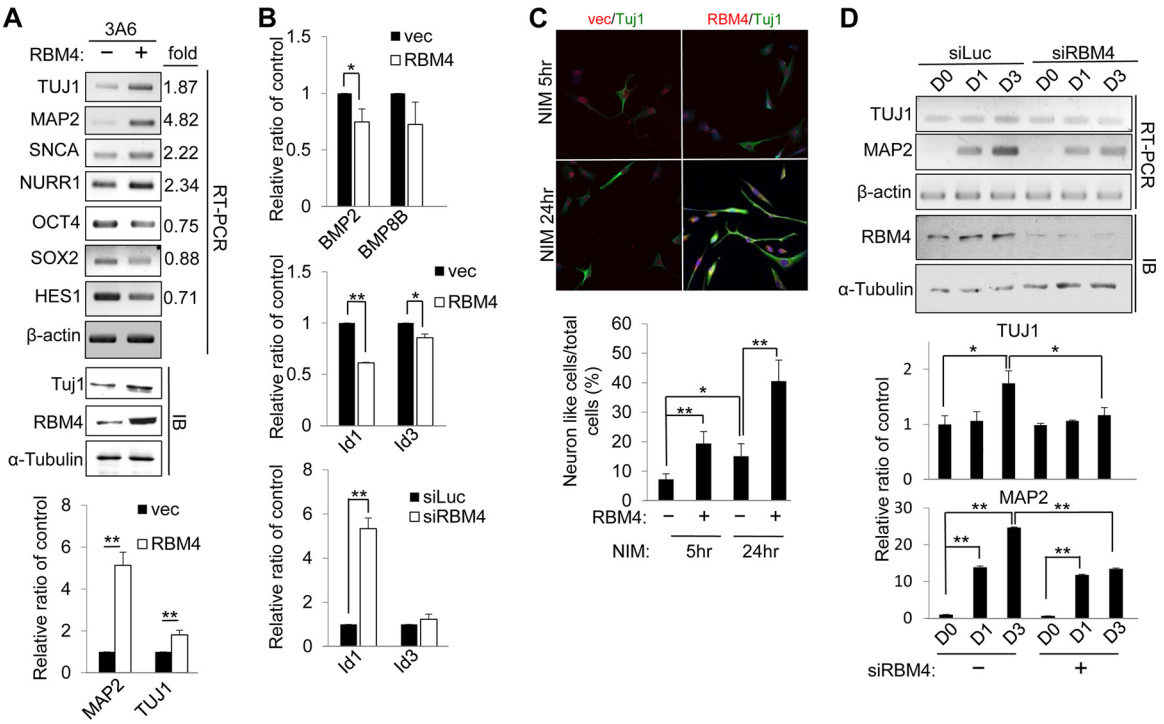

FIG 5 RBM4 promotes neuronal differentiation of MSCs. (A) 3A6 cells were transfected with the empty or FLAG-RBM4 expression vector. Thirty hours after transfection, the expression of the indicated genes was detected by RT-PCR (Table S1). Immunoblotting (IB) was performed using antibodies against Tuj1, RBM4, and α-tubulin. Fold changes are shown to the right. The bar graph shows RT-qPCR data for MAP2 and TUJ1. (B) 3A6 cells were transfected as described for panel A. (Top) The expression of BMP2 and BMP8B was detected by RT-qPCR. 3A6 cells were transfected with the empty or FLAG-RBM4 expression vector (middle) or with siRNA (siRBM4 or siLuc [as a control]) (bottom). The expression of Id1 and Id3 was detected by RT-qPCR. The bar graphs show expression levels of the genes relative to those in the control. (C) 3A6 cells were transfected as described for panel A and then cultured in NIM for 5 or 24 h. Indirect immunofluorescence assay was performed using antibodies against Tuj1 and the FLAG tag. Cells with a Tuj1-positive neurite that was ≥2-fold longer than that of the cell body were defined as neuron-like cells. The bar graph shows the percentage of neuron-like cells in each group. (D) 3A6 cells were transfected with siRBM4 or siLuc. Cells were collected at 24 h posttransfection (D0) or after incubation in NIM for up to 3 days (D1 and D3). TUJ1, MAP2, and β-actin (control) mRNAs were detected by RT-PCR. Immunoblotting (IB) was performed using antibodies against RBM4 and α-tubulin. The bar graph shows levels of each gene relative to control levels. For all bar graphs, the average values and standard deviations were obtained from three independent experiments. *, $P < 0.05$; **, $P < 0.01$.

PKM1 promotes neuronal differentiation and enhances mitochondrial OXPHOS. The above result showing that the relative level of PKM1 increased gradually during MSC neuronal differentiation and was elevated by RBM4 overexpression suggested that PKM1 also promotes neuronal differentiation. Overexpression of PKM1 upregulated the expression of both the TUJ1 and MAP2 genes in noninduced MSCs (Fig. 6A). Immunoblotting confirmed Tuj1 protein expression (Fig. 6A). Moreover, PKM1 enhanced neurite outgrowth under differentiation conditions, as observed with RBM4 (Fig. 6B). The data consistently showed that RBM4 had a higher capacity than that of PKM1 to promote neurite outgrowth at a later postinduction time point (24 h) (Fig. 6B). Perhaps RBM4 promotes the expression of a wider range of neuronal genes than that promoted by PKM1. Furthermore, we overexpressed PKM1 in RBM4 knockdown 3A6 cells and observed that PKM1 was able to restore neuronal gene expression and to suppress negative regulators in the absence of RBM4 (Fig. 6C). This result strengthened the role of PKM1 in neuronal differentiation. Unlike RBM4 and PKM1, PKM2 negatively affected neuronal gene expression and neurite outgrowth (Fig. 6A and B, 24 h).

Next, we assessed whether RBM4 and PKM1 could trigger the change in energy generation from glycolysis to OXPHOS during neuronal differentiation. We used the Seahorse XF analysis system to evaluate the oxygen consumption rate (OCR) in noninduced 3A6 cells. Overexpression of RBM4 or PKM1 resulted in an ~30% higher basal oxygen consumption rate and maximal respiration than those of the control (Fig. 6D). In contrast, PKM2 significantly reduced ATP production, by ~50% (Fig. 6D). This

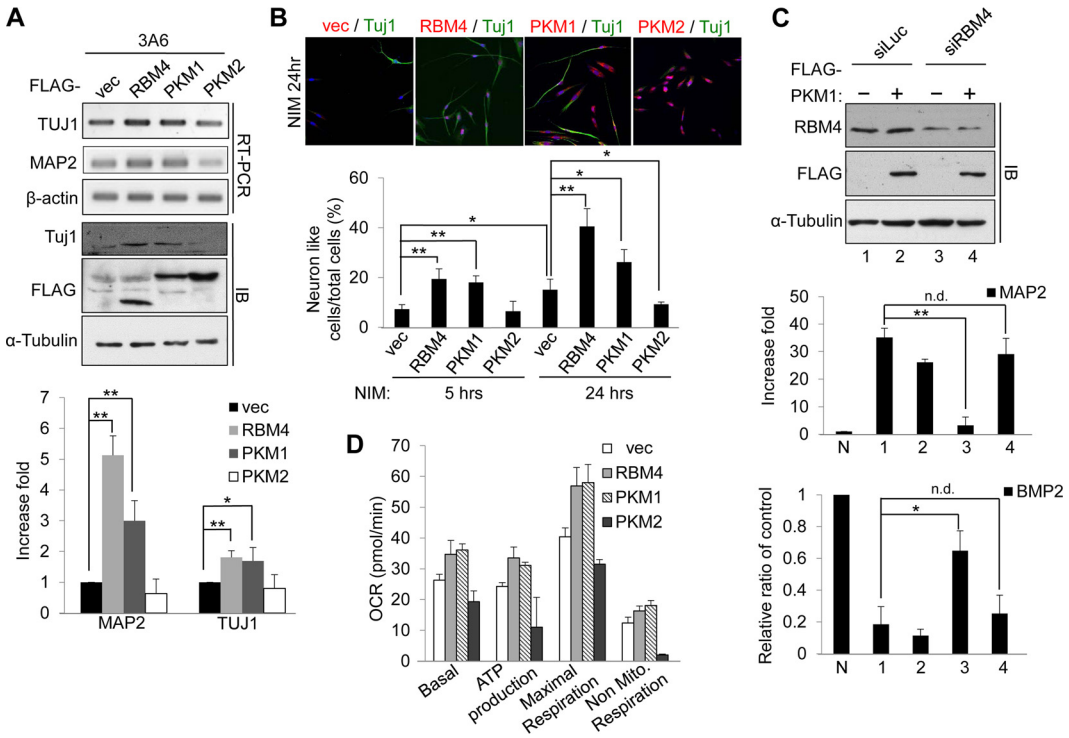

FIG 6 The switch of PKM isoforms contributes to neuronal differentiation of MSCs. (A) 3A6 cells were transfected with an expression vector (empty or FLAG-RBM4, -PKM1, or -PKM2). RT-PCR was performed as described in the legend to Fig. 5D. Immunoblotting (IB) was performed using antibodies against Tuj1, the FLAG tag, and α-tubulin. The bar graph shows RT-qPCR results for MAP2 and TUJ1, as described in the legend to Fig. 5A. (B) 3A6 cells were transfected as described for panel A, followed by culture in NIM for 5 or 24 h. Indirect immunofluorescence staining was performed as described in the legend to Fig. 5C. Representative images of 24-h cultures are shown. The bar graph shows the percentage of neuron-like cells in each group. (C) 3A6 cells were cotransfected with control or RBM4 siRNA and with the empty or FLAG-PKM1 expression vector, followed by neuronal differentiation for 3 days. Bar graphs show the expression of MAP2 (top) and BMP2 (bottom). N, mock-transfected, undifferentiated cells. Average values were obtained from 3 experiments. (D) The oxygen consumption rate of cells transfected as described for panel A was detected by use of the Seahorse XF metabolism analysis system. The bar graph shows the OCR for different cellular metabolic statuses for each group. For all bar graphs, averages and standard deviations were obtained from three independent experiments. *, $P < 0.05$; **, $P < 0.01$; n.d., no significant differences.

observation suggested that RBM4-induced PKM1 is important for altering energy metabolism during neuronal differentiation of MSCs.

RBM4 is involved in the hypoxia-induced switch of PKM splice isoforms and neuronal differentiation. It has been reported that hypoxic conditions or expression of hypoxia-inducible factor 1α (HIF-1α) can promote neuronal differentiation of MSCs (27, 28). Therefore, we cultured noninduced 3A6 cells at 1% oxygen or in the presence of the hypoxia-mimetic agent cobalt chloride ($CoCl_2$) (Fig. 7A). Low oxygen triggered HIF-1α expression, as expected, and increased the levels of neuronal markers (TUJ1 and MAP2 mRNAs) and the RBM4 protein (Fig. 7A). This result indicated that hypoxia was sufficient to initiate neuronal differentiation. Moreover, the increase in RBM4 prompted us to examine whether HIF-1α could induce the expression of RBM4. We transiently overexpressed hemagglutinin (HA)-tagged HIF-1α in 3A6 cells and observed an increase in both RBM4A and RBM4B mRNAs as well as the RBM4 protein (Fig. 7B), suggesting that HIF-1α regulates RBM4 expression through transcriptional control. $CoCl_2$ also induced the expression of the HIF-1α and RBM4 proteins (Fig. 7A, IB panels) as well as TUJ1 and MAP2 mRNAs, consistent with the results from the low-oxygen experiment.

We examined PKM isoform expression in $CoCl_2$-treated 3A6 cells. It has been reported that PKM expression can be induced by HIF-1α (29). Regardless of increased total PKM levels, the ratio of PKM1 to PKM2 was still increased upon $CoCl_2$ treatment, coordinately with the increase in RBM4 (Fig. 7A and C). Next, we depleted RBM4 by use of siRNA in $CoCl_2$-treated 3A6 cells and observed that both the induction of MAP2 and

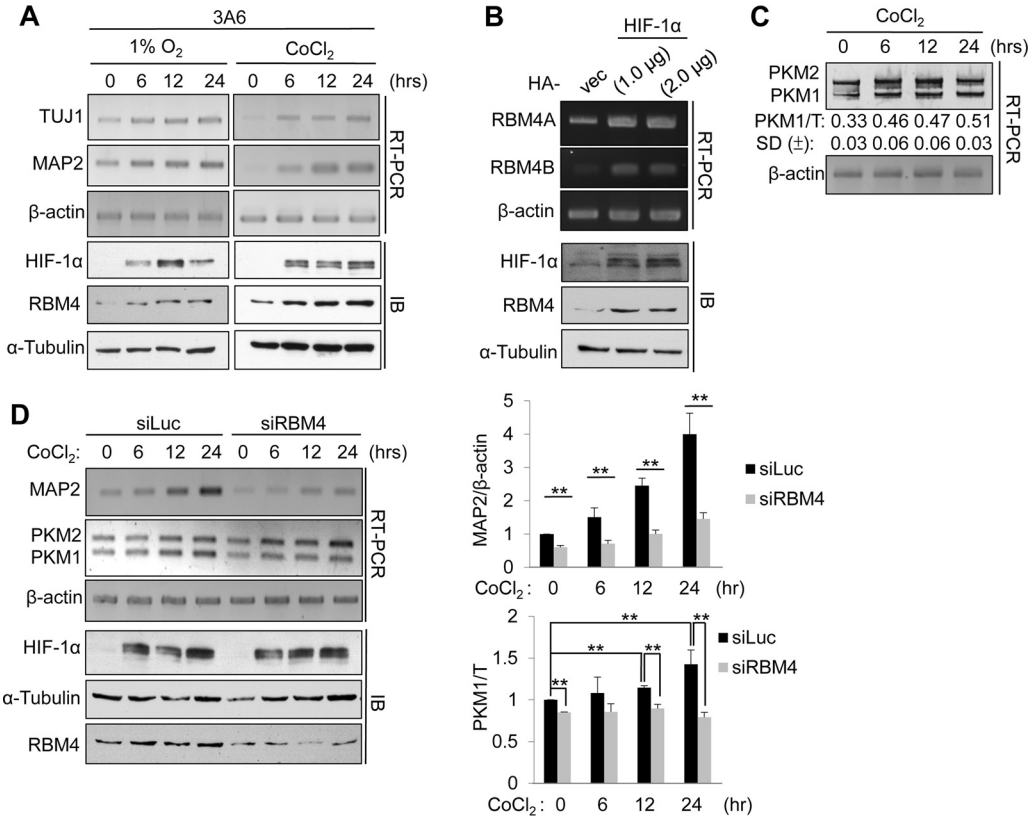

FIG 7 RBM4 is involved in the hypoxia-induced PKM isoform switch. (A) 3A6 cells were incubated under hypoxic conditions (1% O_2) (left) or treated with 200 μM $CoCl_2$ (right) for 6, 12, and 24 h (0 h as a control). RT-PCR was performed as described in the legend to Fig. 5D. (B) 3A6 cells were transfected with empty or HA-tagged HIF-1α vector. RBM4A, RBM4B, and β-actin mRNAs were detected using RT-PCR. (C) 3A6 cells were treated with $CoCl_2$ as described for panel A. PKM isoforms were detected, and ratios of PKM1 to total PKM are shown below the gels, as in Fig. 2. (D) 3A6 cells were transfected with siLuc or siRBM4 for 2 days and then treated with $CoCl_2$ as described for panel A. The expression of MAP2 and PKM isoforms was detected by RT-PCR. Bar graphs show relative MAP2 expression levels (top) and PKM1/total PKM (T) ratios (bottom). Average values and standard deviations were obtained from three independent experiments. **, $P < 0.01$. For panels A, B, and D, immunoblotting (IB) was performed using antibodies against HIF-1α, RBM4, and α-tubulin.

the PKM2-to-PKM1 switch were abolished (Fig. 7D). However, the increase of overall PKM expression was unaffected. This result indicated that RBM4 is essential for hypoxia-induced neuronal differentiation and the PKM isoform switch.

DISCUSSION

The RBM4-mediated PKM isoform shift contributes to neuronal differentiation. In cancer cells, transcriptional activation and a splice isoform switch lead to an increase in the expression of PKM2, which not only contributes to intricate metabolic reprogramming but also acts as a transcriptional activator (18). In most of the developing mouse tissues we examined, we observed a gradual Pkm isoform switch toward Pkm1 (Fig. 1). The prominent Pkm2-to-Pkm1 switch in the embryonic brain echoes the metabolic shift from glycolysis to OXPHOS during neurogenesis (13, 14). MSCs have the potential to differentiate into various cell types that display distinct metabolic properties (7). In this study, we observed that the PKM splice isoform change occurs in both primary MSCs and derived cells (Fig. 3). Our result showing that PKM1 can upregulate neuronal markers and enhance neurite outgrowth (Fig. 6) argues that the splicing change of PKM is not merely a consequence of cell differentiation. A recent report indicated that mitochondrial bioenergetics and function are upregulated during neuronal differentiation (30). Moreover, fine-tuning of metabolic regulation is critical for the function and cell fate decisions of neural stem/progenitor cells (13–16), emphasizing the role of the PKM splicing switch in neurogenesis. Our results reveal, for the first time,

the significance of the RBM4-PKM1 pathway in neuronal differentiation and possibly also brain development, by enhancing the mitochondrial respiratory capacity.

Hypoxia induces neuronal differentiation via the RBM4-mediated PKM isoform shift. MSCs reside in natural niches in which the concentration of oxygen ranges from 1 to 6%. A hypoxic environment is important for MSCs to maintain both the potential for self-renewal and plasticity (31). Nonetheless, it has been reported that hypoxic treatment can promote neuronal differentiation of various stem cells (32). The activated p38 or extracellular signal-regulated kinase (ERK) pathway could upregulate HIF-1α expression of MSCs during hypoxia-induced neuronal differentiation (27). In addition, HIF-1α promotes neuronal differentiation of MSCs by provoking cell cycle arrest (33). We showed that hypoxic treatment induced neuronal gene expression concurrent with an increase in HIF-1α, supporting the idea that hypoxia increases the potential for neuronal differentiation (Fig. 7). Moreover, we observed that HIF-1α induces RBM4 expression at the transcriptional level and demonstrated that RBM4 is essential for the hypoxia-induced PKM isoform switch as well as for neuronal gene expression. A computational search revealed potential HIF-1α/ARNT binding motifs in the promoters of both the RBM4A and RBM4B genes (http://jaspar.genereg.net/cgi-bin/jaspar_db.pl). HIF-1α-induced RBM4 expression also provides a hint regarding the function of RBM4 under other physiological and pathological low-oxygen conditions.

RBM4 regulates PTB isoform expression and suppresses PTB activity in MSCs. The splicing factors hnRNP A1/A2 and PTB regulate PKM pre-mRNA splicing by suppressing exon 9 selection (22), in a manner opposite to that of RBM4 (Fig. 2). PTB regulates a set of alternative splicing events that suppress neuronal differentiation in nonneuronal cells (34). PTB expression can be regulated posttranscriptionally by microRNAs or through alternative splicing-coupled NMD during neuronal differentiation (34, 35). The exon 11-skipping PTB isoform is an NMD-susceptible isoform. By promoting exon 11 skipping, RBM4 downregulates PTB expression during myogenesis and adipogenesis (3, 5). Nevertheless, neither RBM4-induced exon 11 skipping nor cycloheximide-stabilized PTB transcripts were significantly detected in MSCs (Fig. 4). Perhaps NMD activity was compromised during stem cell differentiation (36). Instead, RBM4 could induce the expression of the exon 9-skipping PTB isoform without affecting overall PTB protein expression in MSCs. This isoform has a lower ability to suppress alternative exons of neuronal transcripts during stem cell differentiation into neurons (Fig. 4) (25). Moreover, RBM4 antagonizes the activity of PTB in splicing regulation (Fig. 2). Thus, our finding adds to the known repertoire of RBM4 functions in modulating PTB expression and activity. Perhaps it is necessary to maintain a low level of PTB activity at early stages of stem cell differentiation. While neuronal cell fate is determined, PTB may subsequently and completely be suppressed by microRNAs (35). Together, our past and present results demonstrate that RBM4 suppresses PTB activity via multiple pathways (Fig. 8). RBM4 may fine-tune mRNA isoform expression by inducing a less active PTB isoform as well as antagonizing the activity or function of PTB in stem cells. Finally, the result showing that PTB promotes PKM2 expression provides a hint that PTB acts as a negative regulator of neuronal differentiation. In fact, knockdown of PTB increased the expression of neuronal markers and reduced the expression of the BMP pathway (see Fig. S2 in the supplemental material). Thus, RBM4 and PTB may function oppositely in neuronal differentiation.

This study reveals new and biologically important targets of RBM4 and suggests the potential for RBM4-mediated neuronal differentiation of MSCs in therapies for neurodegenerative diseases.

MATERIALS AND METHODS

Animals and ethics statement. This study was approved by the Institutional Animal Care and Use Committee (IACUC) of Academia Sinica and was compliant with the Taiwan Ministry of Science and Technology guidelines for ethical treatment of animals. Mice were housed and handled according to the IACUC guidelines.

Embryonic mouse tissue isolation and RT-PCR. *Rbm4a* and *Rbm4b* knockout mice were described previously (4). Embryonic mouse brains, hearts, muscles, and pancreases were isolated at embryonic days

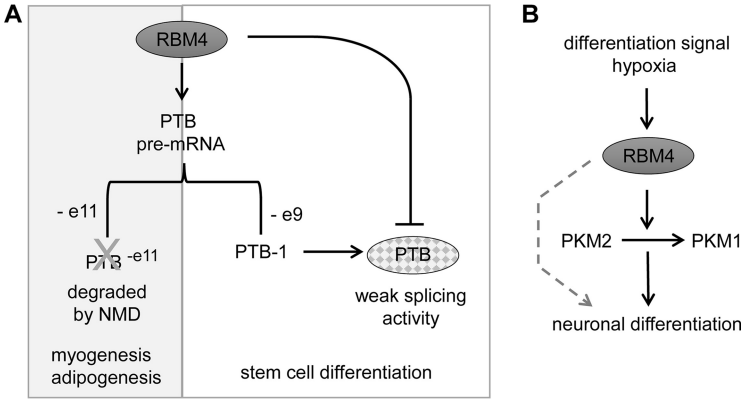

FIG 8 RBM4 modulates neuronal differentiation via alternative splicing regulation. (A) RBM4 modulates alternative splicing of PTB. During myogenesis and adipogenesis, RBM4 promotes the expression of the exon 11-skipping PTB transcript, which is subsequently degraded by NMD. In stem cells, RBM4 induces the skipping of exon 9, resulting in a transcript coding for a functional PTB protein isoform; this isoform exhibits weaker splicing activity than that of full-length PTB. Moreover, RBM4 suppresses the activity of PTB in splicing regulation. (B) Cell differentiation signals or hypoxic treatment can induce RBM4 expression. RBM4 promotes the PKM isoform switch toward PKM1, which increases the mitochondrial respiratory capacity and facilitates neuronal differentiation. The possibility remains that RBM4 promotes neuronal differentiation of MSCs via other pathways (dashed line).

(E) 13.5, 15.5, and 18.5. The brains of *Rbm4* knockout or wild-type embryos were isolated at embryonic day 13.5. Total RNA was extracted by using TRIzol reagent (Thermo Fisher Scientific) following the manufacturer's instructions. For reverse transcription (RT), 2 μg of extracted RNA was treated with RQ1 DNase (Promega), followed by use of a SuperScript III kit (Life Technologies). PCR primer sets are listed in Table S1 in the supplemental material.

Cell culture, neuronal differentiation, and hypoxic induction. Human primary mesenchymal stem cells (MSCs) and derived 3A6 cells have been described previously (24). 3A6 cells immortalized by human papillomavirus 16 (HPV16) E6E7 ectopically express human telomerase reverse transcriptase to gain stem cell-like properties. Primary human MSCs and 3A6 cells were maintained in minimum essential media alpha (αMEM; Gibco) and low-glucose Dulbecco's modified Eagle's medium (LG-DMEM; Gibco), respectively. C2C12 myoblasts, HeLa cells, and HEK293T cells were cultured in DMEM (Gibco) with the same supplement. All the above mediums were supplemented with 10% fetal bovine serum (Gibco), 100 U/ml penicillin, and 100 μg/ml streptomycin (Life Technologies). All cells were cultured in 37°C humidified incubators with 5% CO_2. For neuronal differentiation, primary MSCs or 3A6 cells were seeded at a density of 4,000 cells/cm^2 and induced the next day by use of neuronal induction medium (NIM), containing DMEM without serum and supplemented with 0.1 μM dexamethasone (Sigma), 50 μg/ml ascorbic acid 2-phosphate (Sigma), 50 μM indomethacin (Sigma), and 10 μg/ml insulin (Sigma) (24). The medium was changed every 3 days. For hypoxic induction, 3A6 cells were incubated in a 1% O_2 incubator or treated with 200 μM $CoCl_2$ for up to 24 h.

Immunoblotting and indirect immunofluorescence assay. Immunoblotting was performed using an enhanced chemiluminescence system (Millipore) as described previously (37). Primary antibodies used included polyclonal antibodies against RBM4 (3), α-tubulin (NeoMarkers), the FLAG tag (Sigma-Aldrich), Tuj1 (Biolegend), PTB (Abcam), and HIF-1α (Proteintech). For indirect immunofluorescence assay, transfected cells were induced in NIM for 0, 5, or 24 h and sequentially treated with 3% formaldehyde (Merck) and 0.5% Triton X-100 (Sigma). Fluorescence staining was performed as described previously (37). The cells were observed by using a laser scanning microscope (LSM 700; Zeiss).

Plasmid construction. The expression vectors for FLAG-tagged RBM4 and PTB were described previously (3). To generate the expression vectors for FLAG-tagged PKM1 and PKM2, we performed RT-PCR using 3A6 cell total RNA with specific primers and cloned each cDNA into the pcDNA3.1 vector. To construct the mouse PKM minigene reporter, three genomic DNA fragments, including one from exon 8 to the 5′ part of intron 8, one from the 3′ part of intron 8 to the 5′ part of intron 10, and one from the 3′ part of intron 10 to exon 11, were amplified and ligated, and the resulting DNAs were cloned into pCH110 (GE Healthcare). The mutant PKM reporter was generated by PCR-based mutagenesis. To construct the human PTB minigene, two genomic DNA fragments, one from exon 8 to the 5′ part of intron 9 and the other from the 3′ part of intron 9 to exon 10, were amplified and ligated, and the resulting DNAs were subcloned into pCH110. To construct the FLAG-PTB-1 and FLAG-PTB-4 expression vectors, RT-PCR was performed using 3A6 cell cDNA as the template and one set of primers (Table S1). The corresponding cDNAs were each subcloned into FLAG-containing pCDNA3.1. The expression vector for HA-tagged HIF-1α was obtained from Y.-S. Huang (Academia Sinica, Taipei, Taiwan).

Transfection, *in vivo* splicing assay, and CHX treatment. C2C12 myoblasts, HeLa cells, and HEK293T cells were grown to 80% confluence in 6-well plates and transfected by use of Lipofectamine 2000 (Life Technologies). For 3A6 cells, 2×10^5 cells were seeded in 6-well plates and transfected using GenJet *in vitro* DNA transfection reagent (version II; SignaGen). In general, 0.5 μg of the reporter was

cotransfected with the indicated amounts of the splicing effectors into HEK293 cells for 30 h. Total RNA was isolated for RT-PCR analysis using specific primers (Table S1). To enhance the PCR signals, Southern blotting was performed using specific primers (Table S1) (3). For cycloheximide (CHX) treatment, cells were transfected with the RBM4 expression vector or empty vector for 30 h. The cells were treated with or without CHX for 2 h before being harvested. For knockdown-specific gene expression, 20 pmol of siRNA (Stealth siRNA; Invitrogen) was used to target luciferase (siLuc) or RBM4 (siRBM4) (sense, GCGUA CGCCUUACACCAUGAGUUAU; and antisense, AUAACUCAUGGUGUAAGGCGUACGC).

Cell metabolism assay. 3A6 cells were transfected with a FLAG-protein (RBM4, PKM1, or PKM2) expression vector or empty vector for 30 h. For oxygen consumption rate (OCR) analysis, we exploited the Seahorse system (Agilent Technologies). In brief, 1×10^4 transfected cells were seeded in Seahorse XF 98 plates for 24 h, and the medium was changed 1 h before analysis. Analysis was performed according to the manufacturer's instructions. To gain a complete mitochondrial profile, we used a Mito Stress test kit (Agilent Technologies) following the manufacturer's instructions, sequentially adding oligomycin (1 μM), carbonyl cyanide-4 (trifluoromethoxy) phenylhydrazone (FCCP) (1 μM), and rotenone-antimycin (0.5 μM).

RT-PCR and RT-quantitative PCR (RT-qPCR) assays. Reverse transcription-PCR was performed essentially as described previously (3). Primers used are listed in Table S1 in the supplemental material. To search for potential RBM4 targets during neuronal differentiation of MSCs, we used a neurogenesis PCR array (PAHS-404Z; Qiagen). 3A6 cells were transfected with the FLAG-RBM4 or empty vector for 30 h. Cells were reseeded at a density of 4,000 cells/cm^2 and cultured in NIM for 1 day. Total RNA was extracted for analysis according to the manufacturer's instructions.

Statistical analysis. The Student *t* test was performed to evaluate the significance of differences between experimental groups. Error bars in all graphs indicate standard deviations. *P* values of <0.05 were considered statistically significant.

RNP immunoprecipitation. The FLAG-RBM4 vector was transfected into 3A6 cells for 30 h. Cell lysates were prepared and incubated with anti-FLAG M2 beads (Sigma) in NET-2 buffer (50 mM Tris-HCl, pH 7.4, 150 mM NaCl, and 0.1% NP-40) at 4°C for 2 h. After extensive washing with NET-2 buffer, RNA was extracted by use of TRIzol reagent. RT-PCR was performed using the primers shown in Table S1 in the supplemental material.

EMSA. The CU-rich RNA probe contained a 61-nucleotide (nt) fragment derived from the 3′ end of mouse PKM intron 8 (i.e., 7 to 67 nt upstream of the 3′ splice site). The control contained a 45-nt CU-poor sequence (393 to 437 nt upstream of the 3′ splice site). The probe cDNAs were each subcloned into the pGEM-T vector (Promega). The RNA probes were *in vitro* transcribed from NotI-linearized plasmids by use of T7 RNA polymerase (Promega). Electrophoretic mobility shift assay (EMSA) was performed essentially as described previously (3). Recombinant maltose binding protein (MBP) and MBP-RBM4 were described previously (3). For detection of RNA-protein interactions, 2.8 μg ($\sim$55 pmol) of recombinant MBP-RBM4 was incubated with 5×10^4 cpm of ^{32}P-labeled probe (75 fmol for the CU-rich probe) at 30°C for 30 min. The reactions were analyzed by electrophoresis on a 6% nondenaturing polyacrylamide gel as described previously (3).

SUPPLEMENTAL MATERIAL

Supplemental material for this article may be found at https://doi.org/10.1128/MCB.00466-16.

TEXT S1, PDF file, 0.08 MB.

TEXT S2, PDF file, 0.07 MB.

TEXT S3, PDF file, 0.07 MB.

ACKNOWLEDGMENTS

We thank D. Dhananjaya for recombinant protein and for discussion, Yi-Shuian Huang for an expression vector, and the Core Facility of the Institute of Biomedical Sciences, Academia Sinica, for technical assistance.

C.-H.S. designed and performed the majority of experiments and contributed to manuscript preparation. K.-Y.H. provided mouse embryos and performed RT-qPCR. S.-C.H. provided MSCs and cell lines. W.-Y.T. oversaw the project, designed the experiments, and wrote the manuscript.

We declare that we have no conflicts of interest.

This work was supported by Ministry of Science and Technology grant 104-2321-B-001-066.

REFERENCES

1. Tarn WY, Kuo HC, Yu HI, Liu SW, Tseng CT, Dhananjaya D, Hung KY, Tu CC, Chang SH, Huang GJ, Chiu IM. 2016. RBM4 promotes neuronal differentiation and neurite outgrowth via Numb isoform expression. Mol Biol Cell 27:1676–1683. https://doi.org/10.1091/mbc.E15-11-0798.
2. Wang Y, Chen D, Qian H, Tsai YS, Shao S, Liu Q, Dominguez D, Wang Z. 2014. The splicing factor RBM4 controls apoptosis, proliferation, and migration to suppress tumor progression. Cancer Cell 26:374–389. https://doi.org/10.1016/j.ccr.2014.07.010.
3. Lin JC, Tarn WY. 2011. RBM4 down-regulates PTB and antagonizes its activity in muscle cell-specific alternative splicing. J Cell Biol 193:509–520. https://doi.org/10.1083/jcb.201007131.
4. Lin JC, Yan YT, Hsieh WK, Peng PJ, Su CH, Tarn WY. 2013. RBM4 promotes

pancreas cell differentiation and insulin expression. Mol Cell Biol 33: 319–327. https://doi.org/10.1128/MCB.01266-12.
5. Lin JC, Lu YH, Liu YR, Lin YJ. 9 February 2016. RBM4a-regulated splicing cascade modulates the differentiation and metabolic activities of brown adipocytes. Sci Rep https://doi.org/10.1038/srep20665.
6. Joyce N, Annett G, Wirthlin L, Olson S, Bauer G, Nolta JA. 2010. Mesenchymal stem cells for the treatment of neurodegenerative disease. Regen Med 5:933–946. https://doi.org/10.2217/rme.10.72.
7. Shyh-Chang N, Daley GQ, Cantley LC. 2013. Stem cell metabolism in tissue development and aging. Development 140:2535–2547. https://doi.org/10.1242/dev.091777.
8. Folmes CDL, Dzeja PP, Nelson TJ, Terzic A. 2012. Metabolic plasticity in stem cell homeostasis and differentiation. Cell Stem Cell 11:596–606. https://doi.org/10.1016/j.stem.2012.10.002.
9. Rossi DJ, Jamieson CHM, Weissman IL. 2008. Stems cells and the pathways to aging and cancer. Cell 132:681–696. https://doi.org/10.1016/j.cell.2008.01.036.
10. Facucho-Oliveira JM, Alderson J, Spikings EC, Egginton S, St John JC. 2007. Mitochondrial DNA replication during differentiation of murine embryonic stem cells. J Cell Sci 120:4025–4034. https://doi.org/10.1242/jcs.016972.
11. Takubo K, Nagamatsu G, Kobayashi CI, Nakamura-Ishizu A, Kobayashi H, Ikeda E, Goda N, Rahimi Y, Johnson RS, Soga T, Hirao A, Suematsu M, Suda T. 2013. Regulation of glycolysis by Pdk functions as a metabolic checkpoint for cell cycle quiescence in hematopoietic stem cells. Cell Stem Cell 12:49–61. https://doi.org/10.1016/j.stem.2012.10.011.
12. Chen CT, Shih YR, Kuo TK, Lee OK, Wei YH. 2008. Coordinated changes of mitochondrial biogenesis and antioxidant enzymes during osteogenic differentiation of human mesenchymal stem cells. Stem Cells 26: 960–968. https://doi.org/10.1634/stemcells.2007-0509.
13. Homem CCF, Steinmann V, Burkard TR, Jais A, Esterbauer H, Knoblich A. 2014. Ecdysone and Mediator change energy metabolism to terminate proliferation in Drosophila neural stem cells. Cell 158:874–888. https://doi.org/10.1016/j.cell.2014.06.024.
14. Lange C, Garcia MT, Decimo I, Bifari F, Eelen G, Quaegebeur A, Boon R, Zhao H, Boeckx B, Chang J, Wu C, Le Nobel F, Lambrechts D, Dewerhin M, Kuo CJ, Huttner WB, Carmeliet P. 2016. Relief of hypoxia by angiogenesis promotes neural stem cell differentiation by targeting glycolysis. EMBO J 35:924–941. https://doi.org/10.15252/embj.201592372.
15. Bartesaghi S, Graziano V, Galavotti S, Henriquez NV, Betts J, Saxena J, Deli A, Karlsson A, Martins LM, Capasso M, Nicotera P, Brandner S, De Laurenzi V, Salomoni P. 2015. Inhibition of oxidative metabolism leads to p53 genetic inactivation and transformation in neural stem cells. Proc Natl Acad Sci U S A 112:1059–1064. https://doi.org/10.1073/pnas.1413165112.
16. Bélanger M, Allaman I, Magistretti PJ. 2011. Brain energy metabolism: focus on astrocyte-neuron metabolic cooperation. Cell Metab 14: 724–738. https://doi.org/10.1016/j.cmet.2011.08.016.
17. Zhang Y, Chen K, Sloan SA, Bennett ML, Scholze AR, O'Keeffe S, Phatnani HP, Guarnieri P, Caneda C, Ruderisch N, Deng S, Liddelow SA, Zhang C, Daneman R, Maniatis T, Barres BA, Wu JQ. 2014. An RNA-sequencing transcriptome and splicing database of glia, neurons, and vascular cells of the cerebral cortex. J Neurosci 34:11929–11947. https://doi.org/10.1523/JNEUROSCI.1860-14.2014.
18. Alves-Filho JC, Pålsson-McDermott EM. 21 April 2016. Pyruvate kinase M2: a potential target for regulating inflammation. Front Immunol https://doi.org/10.3389/immu.2016.00145.
19. Taniguchi K, Ito Y, Sugito N, Kumazaki M, Shinohara H, Yamada N, Nakagawa Y, Sugiyama T, Futamura M, Otsuki Y, Yoshida K, Uchiyama K, Akao Y. 2015. Organ-specific PTB1-asociated microRNAs determine expression of pyruvate kinase isoforms. Sci Rep 5:8647. https://doi.org/10.1038/srep08647.
20. David CJ, Chen M, Assanah M, Canoll P, Manley JL. 2010. hnRNP proteins controlled by c-Myc deregulate pyruvate kinase mRNA splicing in cancer. Nature 463:364–368. https://doi.org/10.1038/nature08697.
21. Clower CV, Chatterjee D, Wang Z, Cantley LC, Vander Heiden MG, Krainer AR. 2010. The alternative splicing repressors hnRNP A1/A2 and PTB influence pyruvate kinase isoform expression and cell metabolism. Proc Natl Acad Sci U S A 107:1894–1899. https://doi.org/10.1073/pnas.0914845107.
22. Chen M, David CJ, Manley JL. 2012. Concentration-dependent control of pyruvate kinase M mutually exclusive splicing by hnRNP proteins. Nat Struct Mol Biol 19:346–354. https://doi.org/10.1038/nsmb.2219.
23. Lin JC, Tarn WY. 2005. Exon selection in alpha-tropomyosin mRNA is regulated by the antagonistic action of RBM4 and PTB. Mol Cell Biol 25:10111–10121. https://doi.org/10.1128/MCB.25.22.10111-10121.2005.
24. Tsai CC, Chen CL, Liu HC, Lee YT, Wang HW, Hou LT, Hung SC. 2010. Overexpression of hTERT increases stem-like properties and decreases spontaneous differentiation in human mesenchymal stem cell lines. J Biomed Sci 17:64. https://doi.org/10.1186/1423-0127-17-64.
25. Gueroussov S, Gonatopoulos-Pournatzis T, Irimia M, Raj B, Lin ZY, Gingras AC, Blencowe BJ. 2015. An alternative splicing event amplifies evolutionary differences between vertebrates. Science 349:868–873. https://doi.org/10.1126/science.aaa8381.
26. Nakashima K, Takizawa T, Ochiai W, Yanagisawa M, Hisatsune T, Nakafuku M, Miyazono K, Kishimoto T, Kageyama R, Taga T. 2001. BMP2-mediated alteration in the developmental pathway of fetal mouse brain cells from neurogenesis to astrocytogenesis. Proc Natl Acad Sci U S A 8:5868–5873.
27. Wang Y, Yang J, Li H, Wang X, Zhu L, Fan M, Wang X. 2013. Hypoxia promotes dopaminergic differentiation of mesenchymal stem cells and shows benefits for transplantation in a rat model of Parkinson's disease. PLoS One 8:e54296. https://doi.org/10.1371/journal.pone.0054296.
28. Jeon ES, Shin JH, Hwang SJ, Moon GJ, Bang OY, Kim HH. 2014. Cobalt chloride induces neuronal differentiation of human mesenchymal stem cells through upregulation of microRNA-124a. Biochem Biophys Res Commun 444:581–587. https://doi.org/10.1016/j.bbrc.2014.01.114.
29. Luo W, Hu H, Chang R, Zhong J, Knable M, O'Meally R, Cole RN, Pandey A, Semenza GL. 2011. Pyruvate kinase M2 is a PHD3-stimulated coactivator for hypoxia-inducible factor 1. Cell 145:732–744. https://doi.org/10.1016/j.cell.2011.03.054.
30. Agostini M, Romeo F, Inoue S, Niklisin-Chirou MV, Elia AJ, Dinsdale D, Morone N, Knight RA, Mak TW, Melino G. 8 April 2016. Metabolic reprogramming during neuronal differentiation. Cell Death Differ https://doi.org/10.1038/cdd.2016.36.
31. Mohyeldin A, Garzón-Muvdi T, Quiñones-Hinojosa A. 2010. Oxygen in stem cell biology: a critical component of the stem cell niche. Cell Stem Cell 7:150–161. https://doi.org/10.1016/j.stem.2010.07.007.
32. Vieira HL, Alves PM, Vercelli A. 2011. Modulation of neuronal stem cell differentiation by hypoxia and reactive oxygen species. Prog Neurobiol 93:444–455. https://doi.org/10.1016/j.pneurobio.2011.01.007.
33. Pacary E, Legros H, Valable S, Duchatelle P, Lecocq M, Petit E, Nicole O, Bernaudin M. 2006. Synergistic effect of CoCl(2) and ROCK inhibition on mesenchymal stem cell differentiation into neuron-like cells. J Cell Sci 199:2667–2678.
34. Boutz PL, Stoilov P, Li Q, Lin CH, Chawla G, Ostrow K, Shiue L, Ares M, Jr, Black DL. 2007. A post-transcriptional regulatory switch in polypyrimidine tract-binding proteins reprograms alternative splicing in developing neurons. Genes Dev 21:1636–1652. https://doi.org/10.1101/gad.1558107.
35. Makeyev EV, Zhang J, Carrasco MA, Maniatis T. 2007. The microRNA miR-124 promotes neuronal differentiation by triggering brain-specific alternative pre-mRNA splicing. Mol Cell 27:435–448. https://doi.org/10.1016/j.molcel.2007.07.015.
36. Lou CH, Shao A, Shum EY, Espinoza JL, Huang L, Katam R, Wilkinson MF. 2014. Posttranscriptional control of the stem cell and neurogenic programs by the nonsense-mediated RNA decay pathway. Cell Rep 6:748–764. https://doi.org/10.1016/j.celrep.2014.01.028.
37. Lai MC, Kuo HW, Chang WC, Tarn WY. 2003. A novel splicing regulator shares a nuclear import pathway with SR proteins. EMBO J 22: 1359–1369. https://doi.org/10.1093/emboj/cdg126.